

# Numerical analyses of 2D problems using $Fup_n(x,y)$ basis functions

Vedrana Kozulić and Blaž Gotovac

University of Split, Faculty of Civil Engineering, Matice hrvatske 15, HR-21000 Split, Croatia  
e-mail: vedrana.kozulic@gradst.hr

## SUMMARY

*This paper presents a procedure of numerical modeling of two-dimensional engineering problems using functions  $Fup_n(x,y)$ . They are finite, infinitely derivable functions which belong to a class of Rvachev's basis functions  $R_{bf}$ . The properties of these functions enable hierarchic approach to expansion of the numerical solution base either in the entire domain or its segments.*

*The approximate solution of the problem is assumed in the form of a linear combination of basis functions  $Fup_n(x,y)$ . Instead of traditional discretization into finite elements, here, the entire domain can be analyzed at once, as one fragment. A system of equations is formed by the collocation method in which differential equation of the problem is satisfied in collocation points of a closed domain while boundary conditions are satisfied exactly at the domain boundary. In such a way, the required accuracy of the approximate solution is obtained simply by increasing the number of basis functions. The values of the main solution function and all the values derived from the main solution are calculated in the same points since numerical integration is avoided.*

*This method is tested on the torsion of prismatic bars, plane states and thin plate bending problems. The results of the analyses are compared with the existing exact and relevant numerical solutions. It can be concluded that the fragment collocation method using basis functions  $Fup_n(x,y)$  gives excellent results for elaborated problems either with regard to accuracy or continuity of all fields derived from approximate solutions.*

**Key words:** approximate solution, Rvachev's basis functions, collocation method, fragment.

## 1. INTRODUCTION

This paper presents a new approach to numerical modeling in which the whole domain is considered at once. Namely, in engineering practice, most of the problems are solved in domains the geometry of which can be described by elementary functions. The idea consists of the following: - the geometry of the domain shall be described in the most adequate way independently of the approximate solution base; - the entire domain shall be considered at once as one or several fragments; - an arbitrarily accurate numerical solution shall be obtained by arbitrary increase in the number of basis functions on the fragment; - simultaneously, in the same points the values of the solution function are calculated, e.g. displacements, and all the fields derived from them such as stresses, bending moments, transversal forces, which are generally more interesting than the solution function itself; - all fields derived from the solution function shall be expressed by continuous functions on the domain; - an increase in accuracy of approximate solution is enabled by hierarchic increase of the basis function number on the

fragment or part of the fragment without intrusion into the rest of the domain. In order to fulfil the set goals, a good selection of basis functions shall be done.

Functions, which are implemented in the numerical analyses in this paper, are the  $Fup_n(x,y)$  basis functions. They belong to a class of finite, infinitely derivable functions [1] named after their authors Rvachev's basis functions or, in short,  $R_{bf}$ . The existing knowledge on functions of  $R_{bf}$  class is systemized in Ref. [2], basis functions are transformed into numerically applicable form, and the first steps for their use in practice are realized. These basis functions have good approximation properties as well as a very important property of universality, which enables hierarchic expansion of approximate solution base on the fragment.

Because of infinite derivability of the functions  $Fup_n(x,y)$ , the derivatives of all orders, required by differential equation and boundary conditions, can be used directly in the numerical procedure. Therefore, the collocation method has been applied in the development of numerical models. The collocation method enables efficient, economical and simple procedure. At the same

time, numerical integration is avoided. For purposes of brevity, **Fup Fragment Collocation Method** will be further referred to as **FFCM**.

## 2. FUNCTIONS $Fup_n(x,y)$

Functions  $Fup_n(x)$  belong to a class of Rvachev's basis functions  $R_{bf}$  which are determined as finite solutions of non-homogeneous differential-functional equations [2]. They belong to a space containing algebraic polynomials i.e. algebraic polynomials can be accurately described by linear combinations of mutually displaced basis functions  $Fup_n(x)$ . Index  $n$  denotes the greatest degree of a polynomial which can be expressed accurately in the form of a linear combination of basis functions obtained by displacement of function  $Fup_n(x)$  by a characteristic interval  $2^{-n}$ . When  $n=0$ :

$$Fup_0(x) = up(x) \quad (1)$$

where function  $up(x)$  is the basis function with the support  $[-1, 1]$  and characteristic interval  $\Delta x = 2^0 = 1$  [2]. The function  $Fup_n(x)$  values are calculated using a linear combination of displaced  $up(x)$  functions:

$$Fup_n(x) = \sum_{k=0}^{\infty} C_k(n) up\left(x - 1 - \frac{k}{2^n} + \frac{n+2}{2^{n+1}}\right) \quad (2)$$

where coefficients  $C_k(n)$  are given in Ref. [2]. Function  $Fup_n(x)$  support is determined according to:

$$supp Fup_n(x) = \left[-(n+2)2^{-n-1}; (n+2)2^{-n-1}\right] \quad (3)$$

The basis function for numerical analyses of two dimensional problems is obtained as a Cartesian product of functions (2) by each coordinate axis:

$$Fup_n(x,y) = Fup_n(x) \cdot Fup_n(y) \quad (4)$$

In solving the given problem by the collocation method i.e. solving the partial differential equation of  $n$ -th order and satisfying kinematic and dynamic boundary conditions, the values of all partial derivatives of the function  $Fup_n(x,y)$  shall be known, with  $n$ -th order included. The calculation of all required derivatives of function  $Fup_n(x,y)$  can be written in an algorithm form according to Eq. (4). Figure 1 gives an axonometric presentation of the basis function  $Fup_2(x,y)$  and its partial derivatives.

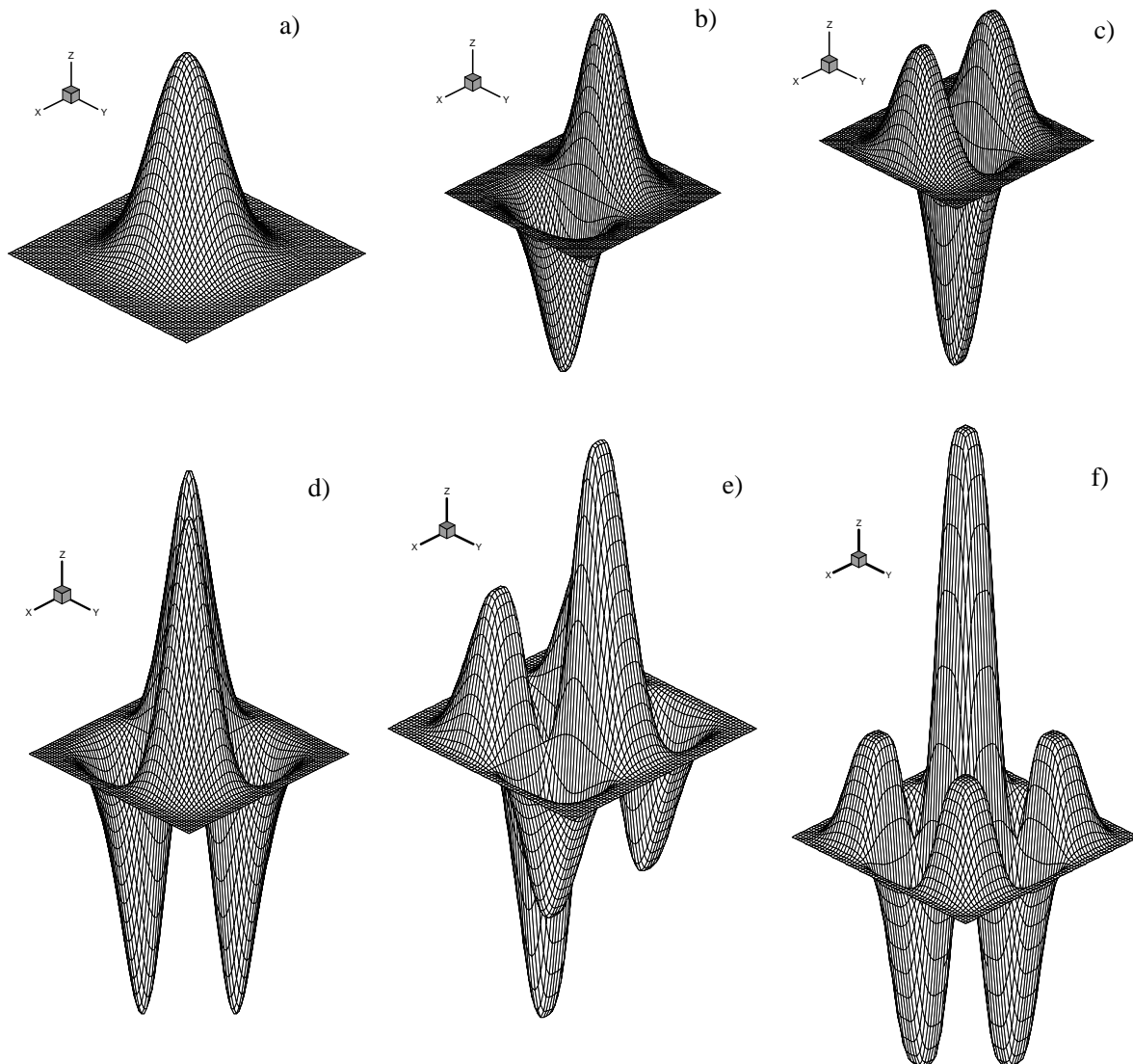


Fig. 1 Basis function  $F \equiv Fup_2(x,y)$ : a)  $F$ ; b)  $\frac{\partial F}{\partial x}$ ; c)  $\frac{\partial^2 F}{\partial x^2}$ ; d)  $\frac{\partial^2 F}{\partial x \partial y}$ ; e)  $\frac{\partial^3 F}{\partial x^2 \partial y}$ ; f)  $\frac{\partial^4 F}{\partial x^2 \partial y^2}$

### 3. FRAGMENT COLLOCATION METHOD

The fragment is the whole observed domain or its significant portion, in a similar sense as a macro-element in the Finite Element Method. However, unlike the macro-element, the fragment does not need to be discretised into smaller segments. Instead, the number of basis functions is arbitrarily increased. In order to obtain smooth solutions on the entire domain by the fragment method with basis functions  $Fup_n(x,y)$ , the collocation method in a point is applied here.

An approximate solution of differential equation:

$$L u(x, y) = f(x, y) \quad (5)$$

with respective boundary conditions is sought by the collocation method in the form of a linear combination:

$$u_N(x, y) = \sum_{i=1}^n \sum_{j=1}^m a_{ij} \cdot \varphi_{ij}(x, y) \quad (6)$$

by solving linear system of equations of  $(n \cdot m) \times (n \cdot m)$  dimension:

$$L u_N(x_k, y_l) = \sum_{i=1}^n \sum_{j=1}^m a_{ij} \cdot L \varphi_{ij}(x_k, y_l) = f(x_k, y_l), \quad (7)$$

$$1 \leq k \leq n, \quad 1 \leq l \leq m$$

where  $L$  is the differential operator,  $\varphi_{ij}$  are basis functions, and  $(x_1, y_1), \dots, (x_n, y_m)$  are collocation points. Function  $u_N(x, y)$  belongs to a  $N$ -dimensional subspace  $X_N$  which represents the set of all linear combinations of basis functions  $\{\varphi_{ij}; 1 \leq i \leq n, 1 \leq j \leq m\}$ . In order to obtain the collocation matrix it is not necessary to perform the numerical integration but only to calculate  $L \varphi_{ij}(x_k, y_l)$  images of the basis functions under the operator  $L$ . Therefore, the collocation method is an efficient alternative procedure for solving partial differential equations.

It is known that the functionality of the collocation method depends on the selection of basis functions  $\varphi_{ij}$  and collocation points  $(x_i, y_j)$ . Prenter [3] proved the stability of the numerical procedure with spline functions when collocation is performed in the so-called natural knots. He developed proofs for the existence and uniformity of the solution and error estimates. Since functions  $Fup_n(x, y)$  can be regarded as splines of an infinite degree, it can be shown that for them it is also optimal to perform the collocation in natural knots of the basis functions, i.e. vertices of the basis functions situated in a closed domain such as for the base in x-direction formed by functions  $Fup_2(x)$  shown in Figure 2.

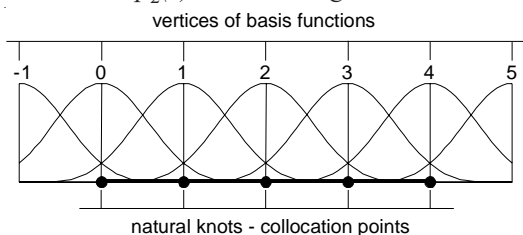


Fig. 2 Collocation points of the base formed by functions  $Fup_2(x)$

This selection of the collocation points provides the simplest numerical procedure; the banded collocation matrix is obtained, which is diagonally dominant and thus well conditioned [4]. This selection also implies equidistance of the collocation points in each coordinate direction.

Taking into consideration the fact that functions  $Fup_n(t)$  are obtained as a linear combination of displaced functions  $up(t)$ , according to Eq. (2), the collocation method error in solving 1D problems can be estimated using the theorem developed by Rvachev [5] for the estimation of an error of approximation of the given function  $f(t) \in C^n[a, b]$ ,  $n \in \mathbb{N}$ , using the functions  $\varphi(t) \in C_0^\infty$ ,  $\text{supp } \varphi = [-1, 1]$ , for each  $h > 0$  for which exists  $c_j^h$ , in the form:

$$\left\| f(t) - \sum_j c_j^h \varphi\left(\frac{t}{h} - 2j^{-n}\right) \right\|_{C[a, b]} \leq C h^n \omega(f^{(n)}, h) \quad (8)$$

In expression (8),  $\varphi(t) \equiv up(t)$ ,  $C$  is the constant,  $h$  is the distance between adjacent collocation points, while  $\omega(f^{(n)}, h)$  is the measure of smoothness of the given function  $f(t)$  and its first  $n$  derivatives in reference to  $h$  value.

### 4. APPLICATIONS

In this paper FFCM has been applied in the analyses of different 2D problems. The numerical model for the analysis of a prismatic bar torsion has been developed. The same problem has been used to illustrate the method of hierarchic expansion of the dimension of basis functions  $Fup_n(x, y)$  vector space. Furthermore, the numerical models for the analyses of the plane states and thin plate bending have also been developed.

#### 4.1 Torsion of prismatic bars

For an isotropic material, the torsion problem is reduced to solving the Poisson's equation:

$$\frac{\partial^2 \Phi(x, y)}{\partial x^2} + \frac{\partial^2 \Phi(x, y)}{\partial y^2} = -2G\vartheta \quad (9)$$

with boundary condition:

$$\Phi|_r = 0 \quad (10)$$

where  $\Phi(x, y)$  is the stress function,  $G$  is the shear modulus, while  $\vartheta$  is the angle of twist per unit length of a bar. Since the torsion problem is described by a partial differential equation of 2<sup>nd</sup> order, functions  $Fup_2(x, y)$  belonging to a class of  $R_{bf}$  functions are selected as basis functions (Figure 1). The approximate solution base is formed on the unit virtual domain defined in the system  $(\xi, \eta)$  according to a scheme shown in Figure 3.

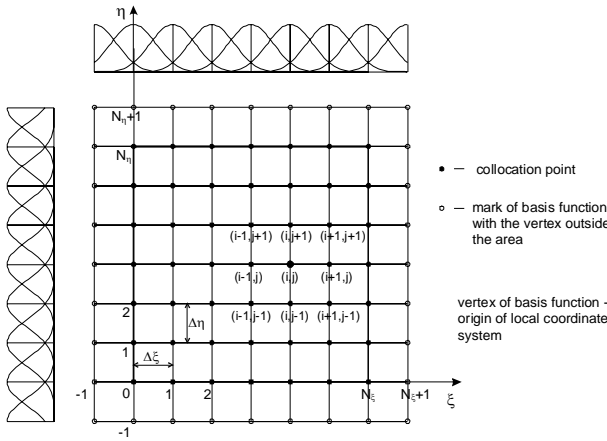


Fig. 3 Distribution of basis functions on the unit virtual domain

Assuming that the cross-section of a bar can be contained within one rectangular fragment of  $a \times b$  dimensions, the differential equation of the problem (9) and boundary condition (10) can be written as:

$$\frac{1}{a^2} \frac{\partial^2 \Phi(\xi, \eta)}{\partial \xi^2} + \frac{1}{b^2} \frac{\partial^2 \Phi(\xi, \eta)}{\partial \eta^2} = -2G\vartheta \quad (11)$$

$$0 \leq \xi \leq 1, \quad 0 \leq \eta \leq 1$$

$$\Phi(\xi, \eta) = 0 \quad \text{for} \quad \xi = 0, \xi = 1, \eta = 0, \eta = 1 \quad (12)$$

The collocation is performed in  $(N_\xi + 1) \times (N_\eta + 1)$  equidistant points, see Figure 3, while the basis functions with the vertex outside the domain are retained so that the basis functions set can be complete. Thus, the governing equation (11) is satisfied in all collocation points of the domain except in the corners; the boundary condition (12) is satisfied in all collocation points of the domain sides while three more conditional equations are satisfied in the corners according to Figure 4. The boundary conditions are therefore exactly satisfied on the domain boundary and not only discretely in collocation points.

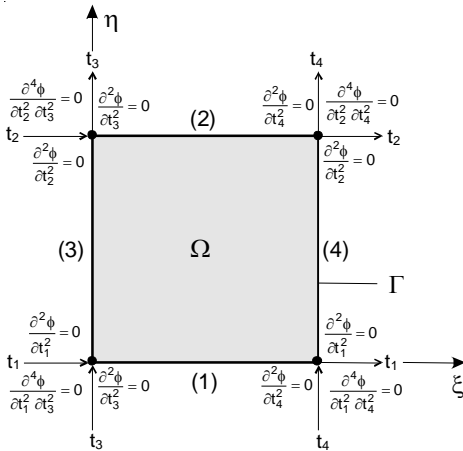


Fig. 4 Designations of domain sides and boundary conditions in corners

Applying the FFCM method to Eqs. (11) and (12) and those in Figure 4, the following collocation equations are obtained:

– for equation (11) within the domain →

$$\sum_{i=-1}^{N_\xi+1} \sum_{j=-1}^{N_\eta+1} C_{ij} \left( \frac{1}{a^2} \frac{\partial^2 F_{ij}(\xi, \eta)}{\partial \xi^2} + \frac{1}{b^2} \frac{\partial^2 F_{ij}(\xi, \eta)}{\partial \eta^2} \right) = -2G\vartheta \quad (13)$$

– for equation (12) on the sides →

$$\sum_{i=-1}^{N_\xi+1} \sum_{j=-1}^{N_\eta+1} C_{ij} \cdot F_{ij}(\xi, \eta) = 0 \quad (14)$$

– for equations given in Figure 4 in corners →

$$\sum_{i=-1}^{N_\xi+1} \sum_{j=-1}^{N_\eta+1} \frac{1}{a^2} C_{ij} \frac{\partial^2 F_{ij}(\xi, \eta)}{\partial \xi^2} = 0$$

$$\sum_{i=-1}^{N_\xi+1} \sum_{j=-1}^{N_\eta+1} \frac{1}{b^2} C_{ij} \frac{\partial^2 F_{ij}(\xi, \eta)}{\partial \eta^2} = 0 \quad (15)$$

$$\sum_{i=-1}^{N_\xi+1} \sum_{j=-1}^{N_\eta+1} \frac{1}{a^2 b^2} C_{ij} \frac{\partial^4 F_{ij}(\xi, \eta)}{\partial \xi^2 \partial \eta^2} = 0$$

In the aforementioned equations  $N_\xi$  and  $N_\eta$  denote a number of partitions of a unit domain in directions  $\xi$  and  $\eta$ , respectively;  $i$  and  $j$  are counters of basis functions in  $\xi$  i.e.  $\eta$  directions, while  $F_{ij}(\xi, \eta)$  is the basis function  $Fup_2(\xi, \eta)$  with the vertex in point  $(i, j)$ . Depending on the number of partitions  $N_\xi$  and  $N_\eta$ , the function  $Fup_2(\xi, \eta)$  support is condensed to  $(4\Delta\xi \times 4\Delta\eta)$ ;  $\Delta\xi = 1/N_\xi$ ,  $\Delta\eta = 1/N_\eta$ . Partial derivatives values of the basis functions in Eqs. (13) to (15) are determined according to the following expression:

$$\frac{\partial^{(m+n)} F_{ij}(\xi, \eta)}{\partial \xi^m \partial \eta^n} = \left( \frac{1}{4\Delta\xi} \right)^m \cdot \left( \frac{1}{4\Delta\eta} \right)^n \cdot Fup_2^{(m+n)} \left( \frac{1}{4\Delta\xi} \xi - \frac{i}{4}, \frac{1}{4\Delta\eta} \eta - \frac{j}{4} \right) \quad (16)$$

Therefore, the solution of the torsion problem on a rectangular domain or domains which can be contained within one rectangular fragment, such as shown in Figure 5, is reduced to solving the system of Eqs. (13)-(14)-(15) of  $(N_\xi + 3) \times (N_\eta + 3)$  equations. The matrix of the system is not symmetrical because the system consists of  $(N_\xi + 1) \times (N_\eta + 1)$  conditional equations in the domain while the remaining equations are boundary conditions at the domain boundary. Since the function  $Fup_2(\xi, \eta)$  is a finite function with the support consisting of  $4 \times 4$  characteristic intervals, the value of the solution function in the collocation point  $(i, j)$  can be expressed by a linear combination of only 9 basis functions (see Fig. 3) in the following form:

$$\Phi(\xi_i, \eta_j) = \sum_{k=i-1}^{i+1} \sum_{l=j-1}^{j+1} C_{kl} \cdot F_{kl}(\xi_i, \eta_j) \quad (17)$$

while the values of all other basis functions in point  $(i, j)$  are equal to zero. In such a way, the banded matrix of the system is obtained.

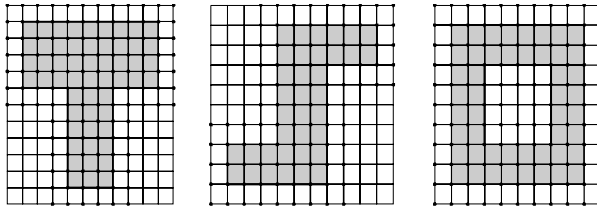


Fig. 5 Different cross-section shapes within rectangular fragment

By solving the system of Eqs. (13)-(14)-(15), the coefficients of a linear combination of the basis functions  $C_{ij}$  are obtained, which can be used to calculate the stress function values  $\Phi$  from Eq. (17) in any point of the cross-section. The shear stress components  $\tau_{xz} = \partial\Phi/\partial y$ ;  $\tau_{yz} = -\partial\Phi/\partial x$ , are calculated with the same accuracy as the main solution using the following expressions:

$$\tau_{xz}(x,y) = \sum_{i=-1}^{N_{\xi}+1} \sum_{j=-1}^{N_{\eta}+1} \frac{1}{b} C_{ij} \cdot \frac{\partial F_{ij}(\xi,\eta)}{\partial \eta} \quad (18)$$

$$\tau_{yz}(x,y) = - \sum_{i=-1}^{N_{\xi}+1} \sum_{j=-1}^{N_{\eta}+1} \frac{1}{a} C_{ij} \cdot \frac{\partial F_{ij}(\xi,\eta)}{\partial \xi}$$

The torsional rigidity of the bar for  $\vartheta=1$  is the double volume under the surface of the stress function  $\Phi$ :

$$C_t = 2 \iint \Phi \, dx \, dy \quad (19)$$

When the collocation method is applied, the integral (19) can be written in the form of a sum:

$$C_t = 2 \sum_{i=0}^{N_{\xi}-1} \sum_{j=0}^{N_{\eta}-1} \underbrace{\int_{\xi_i}^{\xi_i+\Delta\xi} \int_{\eta_j}^{\eta_j+\Delta\eta} \Phi(\xi,\eta) \cdot \det J \cdot d\xi \cdot d\eta}_{I_{(i,j)}} \quad (20)$$

where  $\det J = \sqrt{a \cdot b}$  is the determinant of the Jacobian matrix, while each integral  $I_{(i,j)}$ , see Figure 6, is numerically determined in the form:

$$I_{(i,j)} = \sum_{k=i-1}^{i+2} \sum_{l=j-1}^{j+2} C_{kl} \int_{\xi_i}^{\xi_i+\Delta\xi} \int_{\eta_j}^{\eta_j+\Delta\eta} F_{kl}(\xi,\eta) \det J \, d\xi \, d\eta \quad (21)$$

The values of function  $Fup_2(\xi,\eta)$  integral in Eq. (21) are determined by the Cartesian product of functions  $Fup_2(\xi)$  and  $Fup_2(\eta)$  integrals given in Refs. [2], [4].

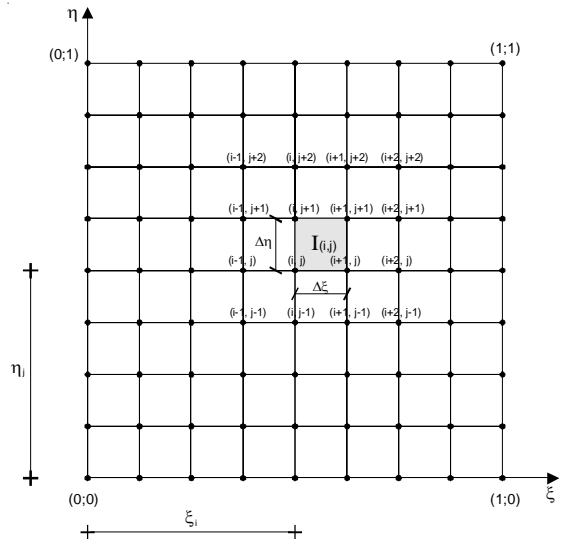


Fig. 6 Scheme for Eq. (21)

#### 4.1.1 Numerical example: analyses using the basis functions $Fup_2(\xi,\eta)$

The torsion of a bar with a square cross-section, made of isotropic material, shown in Figure 7, is analyzed by FFCM using the basis functions  $Fup_2(\xi,\eta)$ . The numerical results are obtained with a different density of collocation points within the domain and shown graphically in Figure 8 complete with the exact solution. An equal number of partitions in each coordinate direction is selected i.e.  $N_{\xi} = N_{\eta} = N$ .

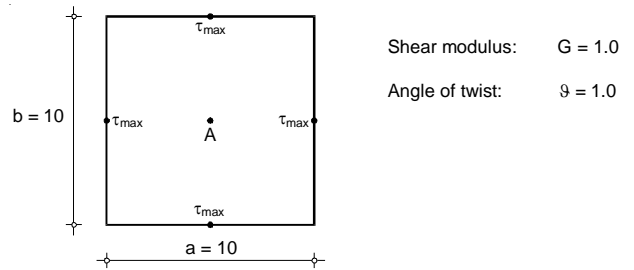


Fig. 7 Square cross-section

Convergence diagrams given in Figure 8 show that the stress function value  $\Phi$  which represents the main solution of the problem, the torsional rigidity which represents the integral value in the cross-section and the maximum shear stress in the point at the boundary have an equally good convergence towards the exact solution.

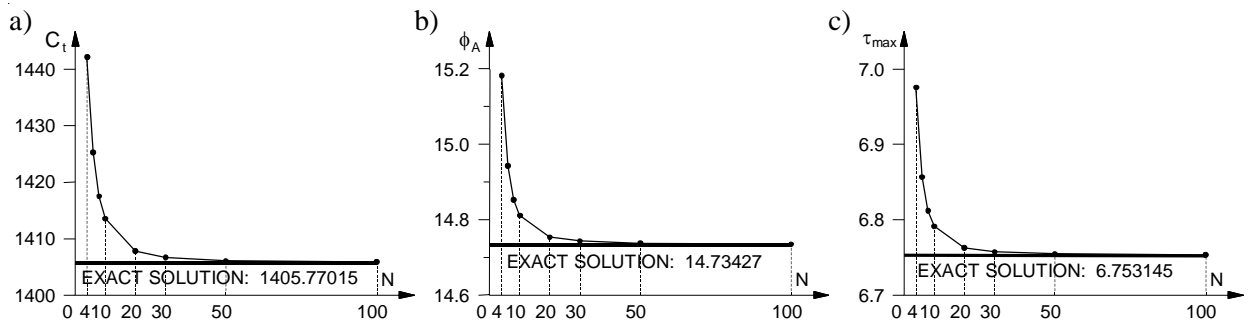


Fig. 8 Convergence of a numerical solution: a) Torsional rigidity; b) Stress function in the middle; c) Maximum shear stress

### 4.1.2 Hierarchic expansion of an approximate solution base

Instead of an increase in the number of basis functions at the same level, the dimension of a vector space can be expanded hierarchically [2], [4].

When  $N_\xi \times N_\eta$  partitions on one fragment are selected i.e.  $(N_\xi + 3) \times (N_\eta + 3)$  the basis functions are mutually displaced by  $\Delta\xi$  in one and  $\Delta\eta$  in the other coordinate direction, as shown in Figure 3, then the selected base is at the “zero level” of approximation. The hierarchic expansion of the vector space dimension is obtained by adding displaced and compressed basis functions. At the first level, functions  $Fup_2(\xi, \eta)$  are added, displaced by  $\Delta\xi/2$ ;  $\Delta\eta/2$  in reference to the functions of the zero level and compressed to a length of the support  $(2\Delta\xi) \times (2\Delta\eta)$ . At the second level, the added basis functions are displaced by  $\Delta\xi/4$ ;  $\Delta\eta/4$  in reference to the “zero level” with the length of the support  $(\Delta\xi \times \Delta\eta)$ , which is  $1/4$  of the length of the basis functions support at the zero level. At higher levels of approximation, the base is built by analogy. Figure 9 shows the distribution of collocation points, in which the vertices of the basis functions are at the zero, first and second levels of approximation. The compression of the functions to  $1/2$  of the support from the preceding level is the consequence of the basic properties of the basis functions [2].

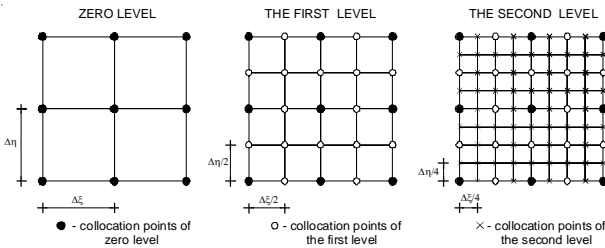


Fig. 9 Hierarchic expansion of a vector space of functions  $Fup_2(\xi, \eta)$

The numerical tests [4] for different densities of collocation points showed that it is sufficient to satisfy the boundary conditions with the basis functions of the zero level while the basis functions of higher levels correct the solution. It means that, for the torsion problem, only the collocation form of the differential equation of the problem will be changed in the system of Eqs. (13)-(14)-(15). For the second level of approximation e.g., in the collocation point within the domain, the following equation will be written instead of Eq. (13):

$$\begin{aligned} & \sum_{i=1}^{N_\xi+1} \sum_{j=1}^{N_\eta+1} C_{ij} \left( \frac{1}{a^2} \frac{\partial^2 F_{ij}(\xi, \eta)}{\partial \xi^2} + \frac{1}{b^2} \frac{\partial^2 F_{ij}(\xi, \eta)}{\partial \eta^2} \right) + \\ & + \sum_{i_1=1}^{N_{\xi_1}} \sum_{j_1=1}^{N_{\eta_1}} D_{i_1 j_1} \left( \frac{1}{a^2} \frac{\partial^2 F_{i_1 j_1}(\xi, \eta)}{\partial \xi^2} + \frac{1}{b^2} \frac{\partial^2 F_{i_1 j_1}(\xi, \eta)}{\partial \eta^2} \right) + \\ & + \sum_{i_2=1}^{N_{\xi_2}} \sum_{j_2=1}^{N_{\eta_2}} E_{i_2 j_2} \left( \frac{1}{a^2} \frac{\partial^2 F_{i_2 j_2}(\xi, \eta)}{\partial \xi^2} + \frac{1}{b^2} \frac{\partial^2 F_{i_2 j_2}(\xi, \eta)}{\partial \eta^2} \right) = -2G\theta \end{aligned} \quad (22)$$

where coefficients  $C_{ij}$  belong to the basis functions of the zero level,  $D_{i_1 j_1}$  to the basis functions of the first level while  $E_{i_2 j_2}$  belong to the basis functions of the second level. The unknown coefficients of the linear combination are determined by solving the system of equations, which can be written in the matrix form using the blocks:

$$\begin{array}{l} \text{ZERO LEVEL} \rightarrow \\ \text{THE FIRST LEVEL} \rightarrow \\ \text{THE SECOND LEVEL} \rightarrow \end{array} \begin{array}{c} \text{ZERO} \\ \text{LEVEL} \\ \text{---} \\ \text{1ST} \\ \text{LEVEL} \\ \text{---} \\ \text{2ND} \\ \text{LEVEL} \end{array} \begin{array}{ccc} AA & AB & AC \\ BA & BB & BC \\ CA & CB & CC \end{array} \cdot \begin{array}{c} C_{ij} \\ D_{i_1 j_1} \\ E_{i_2 j_2} \end{array} = \begin{array}{c} RA \\ RB \\ RC \end{array} \quad (23)$$

The procedure of hierarchic expansion of an approximate solution base is appropriate for computer programming. It can be applied to the entire given domain or only to a part of the domain e.g. at concentrated load locations, for singularities such as concave breaks in the edge where the stress concentration occurs, or in the plastification zones in elasto-plastic analyses [4].

### Example

The effect of hierarchic increase in a number of basis functions will be illustrated on the example of torsion of a bar with a square cross-section analyzed in Section 4.1.1. Figure 10 shows the convergence diagrams of the numerical solution for torsional rigidity value when the number of basis functions increases at the zero level only, and when the approximate solution base is expanded with basis functions of the first and second level. It can be observed that much better numerical solution is obtained with the same total number of basis functions, if a hierarchic approach is applied than when all basis functions belong to a zero level.

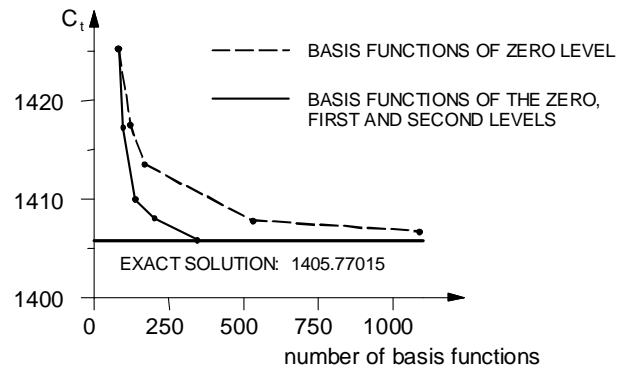


Fig. 10 Diagrams of convergence of torsional rigidity value

4.1.3 Example: analyses using basis functions

$$Fup_4(\xi, \eta)$$

The essence of the **Fup Fragment Collocation Method** is that the density of the basis functions increases on one fragment until an arbitrarily exact solution is obtained. Greater accuracy of a numerical solution can be obtained by an increase in the number of the same basis functions in the given domain, as illustrated in Section 4.1.1. The procedure of hierarchic expansion of the approximate solution base is also possible, as described in Section 4.1.2. FFCM also provides the possibility to select degree  $n$  of the basis functions  $Fup_n(\xi, \eta)$  in solving the given problem. Thus, for solving the torsion problem (9)-(10), the basis functions  $Fup_2(\xi, \eta)$  are selected. However, the basis functions of higher degree can be selected e.g. functions  $Fup_4(\xi, \eta)$  [2], [4], the linear combination of which can be used to describe exactly the polynomial of the 4-th degree on a characteristic interval  $2^{-4}$ . As an illustration, the same square cross-section as in Section 4.1.1 is analyzed here using the functions  $Fup_4(\xi, \eta)$ . The comparison of solutions is given in Table 1.

Table 1. Torsion of a bar with a square cross-section

$Fup_2(\xi, \eta)$			$Fup_4(\xi, \eta)$		
Number of coll. points ( $N+1$ ) $\times$ ( $N+1$ )	Stress function $\Phi_{max}$	Torsional rigidity $C_t$	Number of coll. points ( $N+1$ ) $\times$ ( $N+1$ )	Stress function $\Phi_{max}$	Torsional rigidity $C_t$
$N=4$	15.1826	1442.16	$N=4$	14.7449	1406.88
$N=8$	14.8532	1417.49	$N=8$	14.7351	1405.90
$N=20$	14.7536	1407.79	$N=16$	14.7343	1405.78
$N=100$	14.7350	1405.85	$N=32$	14.7343	1405.77
Exact solution	14.7343	1405.77	Exact solution	14.7343	1405.77

4.1.4 Analyses of curvilinear domains using FFCM

FFCM can be applied successfully to curvilinear domains, too. The surface of the given domain will be described so that the mapping matrix and all required partial derivatives of elements of the inverse mapping matrix can be found in each point of the domain. It is important that the surface can be easily and accurately divided into mutually equal partitions in each coordinate direction in order to fulfill the requirement of equidistance of collocation points on the fragment.

The parametric form is extremely adequate for the description of surfaces and, using the Coons formulation, [6] and [4], can be written in the following form:

$$P(\xi, \eta) = \begin{bmatrix} (1-\xi) & \xi \end{bmatrix} \begin{bmatrix} Q(0, \eta) \\ Q(1, \eta) \end{bmatrix} + \begin{bmatrix} Q(\xi, 0) & Q(\xi, 1) \end{bmatrix} \begin{bmatrix} 1-\eta \\ \eta \end{bmatrix} - \begin{bmatrix} (1-\xi) & \xi \end{bmatrix} \begin{bmatrix} Q(0, 0) & Q(0, 1) \\ Q(1, 0) & Q(1, 1) \end{bmatrix} \begin{bmatrix} 1-\eta \\ \eta \end{bmatrix} \quad (24)$$

where  $Q(0,0)$ ,  $Q(0,1)$ ,  $Q(1,0)$  and  $Q(1,1)$  are position vectors at the four corners while  $Q(\xi,0)$ ,  $Q(\xi,1)$ ,  $Q(0,\eta)$  and  $Q(1,\eta)$  are four boundary curves, see Figure 11. Changing the parameters  $\xi$  and  $\eta$  in equal steps on the interval  $[0,1]$ , using Eq. (24), the equidistant collocation points are obtained within the given domain.

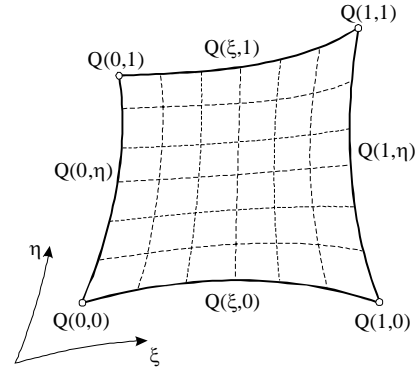


Fig. 11 A Coons surface patch

Thus, for curvilinear domains, the partial differential equation of the torsion problem (9) has the following collocation form:

$$\sum_{i=-1}^{N_\xi+1} \sum_{j=-1}^{N_\eta+1} C_{ij} \cdot \left[ FXX \frac{\partial^2 F_{ij}(\xi, \eta)}{\partial \xi^2} + FXE \frac{\partial^2 F_{ij}(\xi, \eta)}{\partial \xi \partial \eta} + FEE \frac{\partial^2 F_{ij}(\xi, \eta)}{\partial \eta^2} + FX \frac{\partial F_{ij}(\xi, \eta)}{\partial \xi} + FE \frac{\partial F_{ij}(\xi, \eta)}{\partial \eta} \right] = -2G\theta \quad (25)$$

where:

$$FXX = \left( \frac{\partial \xi}{\partial x} \right)^2 + \left( \frac{\partial \xi}{\partial y} \right)^2 ; \quad FEE = \left( \frac{\partial \eta}{\partial x} \right)^2 + \left( \frac{\partial \eta}{\partial y} \right)^2$$

$$FXE = 2 \cdot \left( \frac{\partial \xi}{\partial x} \frac{\partial \eta}{\partial x} + \frac{\partial \xi}{\partial y} \frac{\partial \eta}{\partial y} \right)$$

$$FX = \frac{\partial \xi}{\partial x} \frac{\partial \left( \frac{\partial \xi}{\partial x} \right)}{\partial \xi} + \frac{\partial \eta}{\partial x} \frac{\partial \left( \frac{\partial \xi}{\partial x} \right)}{\partial \eta} + \frac{\partial \xi}{\partial y} \frac{\partial \left( \frac{\partial \xi}{\partial y} \right)}{\partial \xi} + \frac{\partial \eta}{\partial y} \frac{\partial \left( \frac{\partial \xi}{\partial y} \right)}{\partial \eta}$$

$$FE = \frac{\partial \xi}{\partial x} \frac{\partial \left( \frac{\partial \eta}{\partial x} \right)}{\partial \xi} + \frac{\partial \eta}{\partial x} \frac{\partial \left( \frac{\partial \eta}{\partial x} \right)}{\partial \eta} + \frac{\partial \xi}{\partial y} \frac{\partial \left( \frac{\partial \eta}{\partial y} \right)}{\partial \xi} + \frac{\partial \eta}{\partial y} \frac{\partial \left( \frac{\partial \eta}{\partial y} \right)}{\partial \eta} \quad (26)$$

Partial derivatives of elements of the inverse mapping matrix in Eq. (26) are determined by derivation of parametric equations of a surface (24), while partial derivatives of basis functions are determined according to Eq. (16).

**Example**

The torsion of a bar with a cross-section in the form of an eccentric ring, shown in Figure 12, is analyzed by the FFCM. An analytic solution exists for this shape of a cross-section [7].

The entire cross-section is considered as one fragment. The real domain is mapped into a virtual unit domain using the expression (24) where the sides of the fragment (1) and (2) (see Figure 13) are described using the parametric equations of a circle [4]; sides (3) and (4) overlap in a real domain.

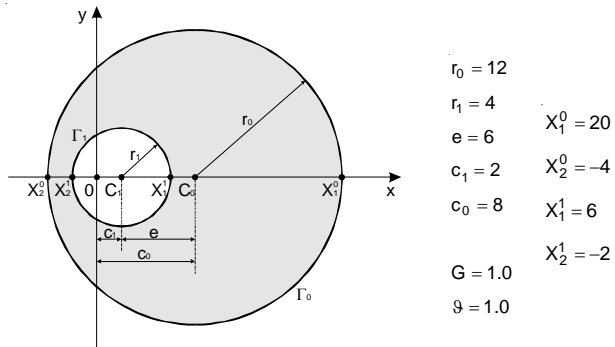


Fig. 12 Cross-section geometry - eccentric ring

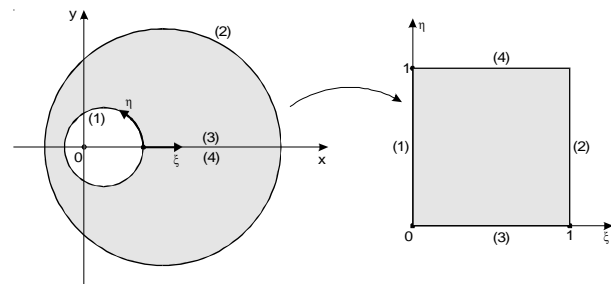


Fig. 13 Mapping of the given fragment from real into virtual unit domain

The convergence of the torsional rigidity value  $C_t$  and the stress function value  $\Phi$  on the inner boundary  $\Gamma_1$ , with an increase in the number of collocation points, is given in Table 2.

Table 2. Comparison of the results for an eccentric ring

Number of collocation points $(N_\xi+1) \times (N_\eta+1)$	$\Phi _{\Gamma_1}$	$\frac{\Phi - \Phi_{exact}}{\Phi_{exact}}$	$C_t$	$\frac{C_t - C_{t, exact}}{C_{t, exact}}$
$N_\xi=10, N_\eta=20$	41.387	5.32 %	28345.72	2.57 %
$N_\xi=20, N_\eta=40$	40.279	2.50 %	27976.24	1.24 %
$N_\xi=50, N_\eta=100$	39.649	0.90 %	27768.75	0.48 %
$N_\xi=100, N_\eta=200$	39.445	0.38 %	27701.30	0.24 %
Exact solution	39.297	—	27634.63	—

The results of numerical analyses are presented graphically in Figure 14.

**4.2 Plane problems**

The system of partial differential equations of the equilibrium:

$$\frac{\partial \sigma_{xx}}{\partial x} + \frac{\partial \tau_{xy}}{\partial y} + F_x = 0 \tag{27}$$

$$\frac{\partial \tau_{xy}}{\partial x} + \frac{\partial \sigma_{yy}}{\partial y} + F_y = 0$$

using the behaviour law written in a matrix form:

$$\begin{Bmatrix} \sigma_{xx} \\ \sigma_{yy} \\ \tau_{xy} \end{Bmatrix} = \frac{Et}{1-\nu^2} \begin{bmatrix} 1 & \nu & 0 \\ \nu & 1 & 0 \\ 0 & 0 & \frac{1-\nu}{2} \end{bmatrix} \cdot \begin{Bmatrix} \frac{\partial u}{\partial x} \\ \frac{\partial v}{\partial y} \\ \frac{\partial u}{\partial y} + \frac{\partial v}{\partial x} \end{Bmatrix} \tag{28}$$

can be transformed into an analogue system of differential equations expressed through displacements  $u$  and  $v$ :

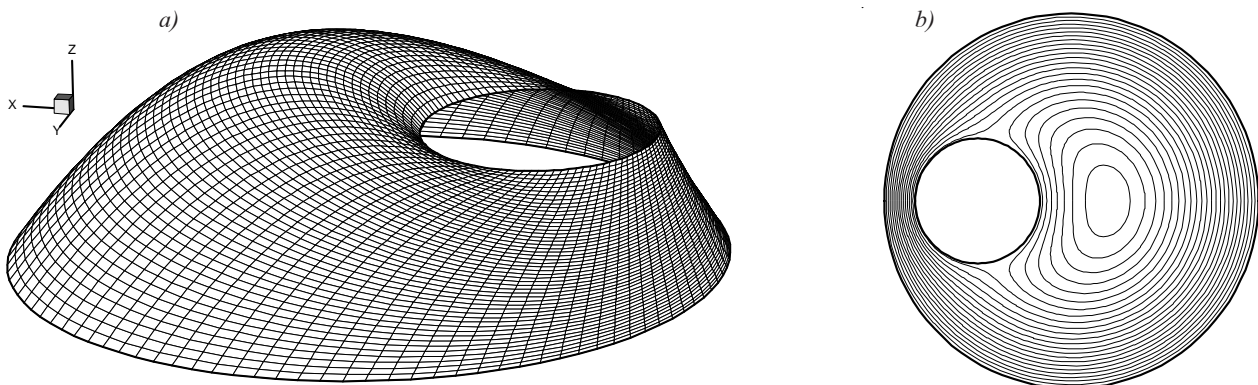


Fig. 14 a) Stress function surface  $\Phi(x,y)$ ; b) Isolines of stress function  $\Phi(x,y)$

$$\frac{\partial^2 u}{\partial x^2} + \frac{1-\nu}{2} \frac{\partial^2 u}{\partial y^2} + \frac{1+\nu}{2} \frac{\partial^2 v}{\partial x \partial y} + \frac{1-\nu^2}{Et} F_x = 0$$

$$\frac{\partial^2 v}{\partial y^2} + \frac{1-\nu}{2} \frac{\partial^2 v}{\partial x^2} + \frac{1+\nu}{2} \frac{\partial^2 u}{\partial x \partial y} + \frac{1-\nu^2}{Et} F_y = 0$$

(29)

In expressions (27), (28) and (29),  $E$  is Young's modulus,  $\nu$  is Poisson's coefficient,  $t$  is thickness of the model while  $F_x$  and  $F_y$  are the components of volumetric forces.

Figure 15 shows the plane stress model with boundary conditions on the supported, free and loaded part of the boundary.

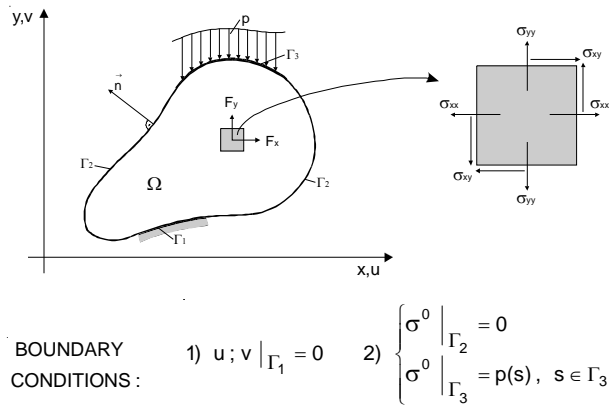


Fig. 15 Plane stress model

By the collocation method, the system of equations is solved directly. The basis functions  $Fup_2(\xi, \eta)$  will be used, similarly as for the torsion problem. Unlike the torsion, there are two degrees of freedom, which means that for each basis function two coefficients of a linear combination must be found. Therefore, an approximate solution of the problem (29) is sought in the form of linear combinations:

$$\tilde{u}(x, y) = \sum_{i=-1}^{N_\xi+1} \sum_{j=-1}^{N_\eta+1} C_{ij} \cdot F_{ij}(\xi, \eta)$$

$$\tilde{v}(x, y) = \sum_{i=-1}^{N_\xi+1} \sum_{j=-1}^{N_\eta+1} D_{ij} \cdot F_{ij}(\xi, \eta)$$

(30)

where  $F_{ij}(\xi, \eta)$  is the basis function  $Fup_2(\xi, \eta)$  with the vertex in the collocation point  $(i, j)$ . The unknown coefficients  $C_{ij}$  and  $D_{ij}$  are determined by solving the system consisting of  $2 \times [(N_\xi+3) \times (N_\eta+3)]$  collocation equations.

### Example

FFCM is applied to analyses of a cantilever wall beam with the concentrated load  $P$  as shown in Figure 16. In accordance with the known analytic solution [8], it is assumed that force  $P$  is distributed at the end cross-section  $x=l$ , according to the same parabolic law for the

variation of shear stresses  $\tau_{xy}$ . The presented support is assumed because the theoretically required assumptions on complete clamping can not be fulfilled completely in reality.

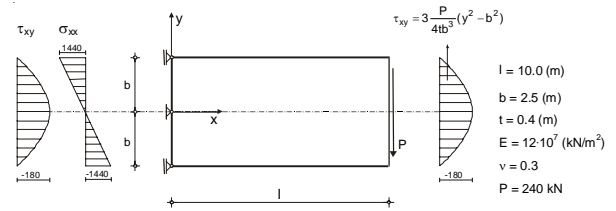


Fig. 16 Cantilever loaded with a force P

In the numerical model, using the FFCM, the entire cantilever is considered as one fragment. All the given kinematic and dynamic boundary conditions are set on the sides of the domain and its corners according to Figure 17.

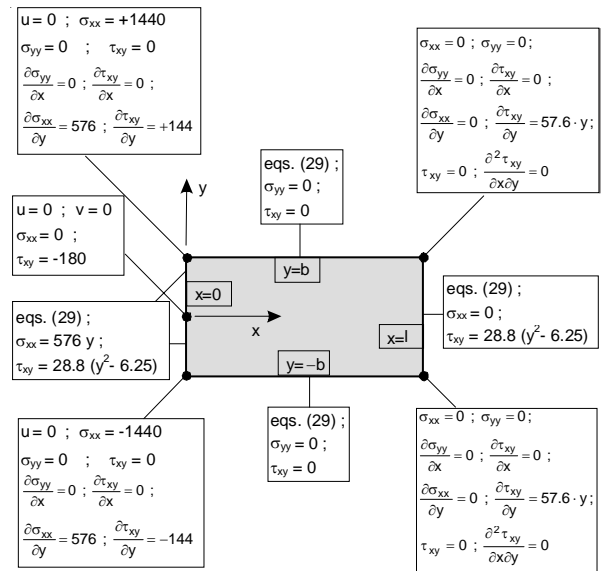


Fig. 17 Conditional equations in collocation points at the domain boundary

In order to evaluate the numerical solution obtained by the FFCM, the selected example has been analyzed using the Finite Element Method. Isoparametric 8-node finite elements have been used with the discretization of  $16 \times 16$  finite elements. The comparison of the obtained numerical solutions with the analytical ones is given in Table 3.

Table 3. Cantilever wall beam - comparison of results

METHOD		Displacements in the point $x = l, y = -b$		
		u	v	
FFCM	N = 4	-0.600	-1.88812	
	N = 8	-0.600	-1.87828	
	N = 16	-0.600	-1.87582	
	N = 32	-0.600	-1.87520	
FEM		16x16 F.E.	-0.599	-1.87254
Exact solution			-0.600	-1.87500

Smooth functions of all fields derived from the main solution i.e. displacements are obtained using the basis functions  $Fup_2(\xi, \eta)$ . The results of the numerical analyses obtained by FFCM are shown graphically in Figures 18, 19 and 20: displacement vectors in the collocation points of a cantilever, isolines of stresses  $\sigma_{xx}$  and trajectories of compressive and tensile stresses.

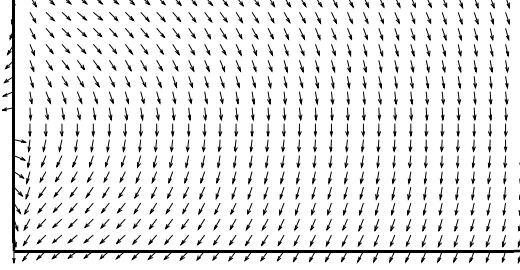


Fig. 18 Displacement vectors

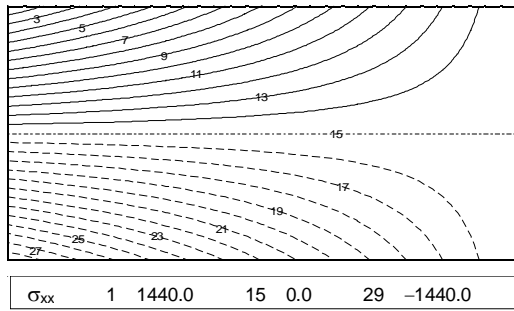


Fig. 19 Isolines of stresses  $\sigma_{xx}$

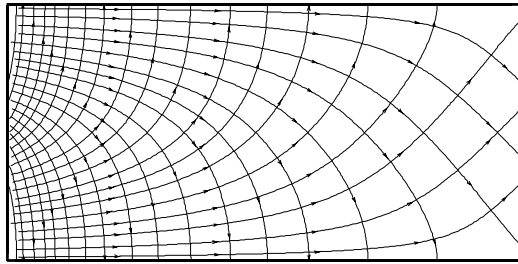


Fig. 20 Stress trajectories

### 4.3 Bending of thin plates

Bending of thin, homogeneous and isotropic plates is described by the following differential equation:

$$\nabla^4 w = \frac{p(x, y)}{D} \quad (31)$$

and the respective boundary conditions, where  $D$  is flexural rigidity,  $p$  is normal pressure while  $w$  is deflection of the plate.

Since plate behaviour is described by a partial differential equation of the fourth order, in numerical modeling using the FFCM, it is most adequate to select  $Fup_4(\xi, \eta)$  as basis functions. The basis function  $Fup_4(\xi, \eta)$  has 6 characteristic intervals for each coordinate direction, Ref. [4], so that the schematic presentation of the approximate solution base, formed on the unit virtual domain, looks as shown in Figure 21. Two series of vertex points are outside the domain, exactly as required in order to satisfy exactly all the given boundary conditions in collocation points on the sides and in the corners of the domain.

Therefore, an approximate solution of the problem is sought using  $(N_\xi+1) \times (N_\eta+1)$  collocation points i.e.  $(N_\xi+5) \times (N_\eta+5)$  basis functions. When the FFCM is applied to a rectangular plate of  $a \times b$  size, the collocation form of the differential equation (31) is:

$$\sum_{i=-2}^{N_\xi+2} \sum_{j=-2}^{N_\eta+2} C_{ij} \left[ \frac{1}{a^4} \frac{\partial^4 F_{ij}(\xi, \eta)}{\partial \xi^4} + \frac{2}{a^2 \cdot b^2} \frac{\partial^4 F_{ij}(\xi, \eta)}{\partial \xi^2 \partial \eta^2} + \frac{1}{b^4} \frac{\partial^4 F_{ij}(\xi, \eta)}{\partial \eta^4} \right] = \frac{p}{D} \quad (32)$$

In Eq. (32)  $F_{ij}(\xi, \eta)$  is the basis function  $Fup_4(\xi, \eta)$  with the vertex in point  $(i, j)$ , while partial derivatives of basis functions are determined according to the following expression:

$$\frac{\partial^{(m+n)} F_{ij}(\xi, \eta)}{\partial \xi^m \partial \eta^n} = \left( \frac{1}{16\Delta\xi} \right)^m \cdot \left( \frac{1}{16\Delta\eta} \right)^n \cdot Fup_4^{(m+n)} \left( \frac{1}{16\Delta\xi} \xi - \frac{i}{16}, \frac{1}{16\Delta\eta} \eta - \frac{j}{16} \right) \quad (33)$$

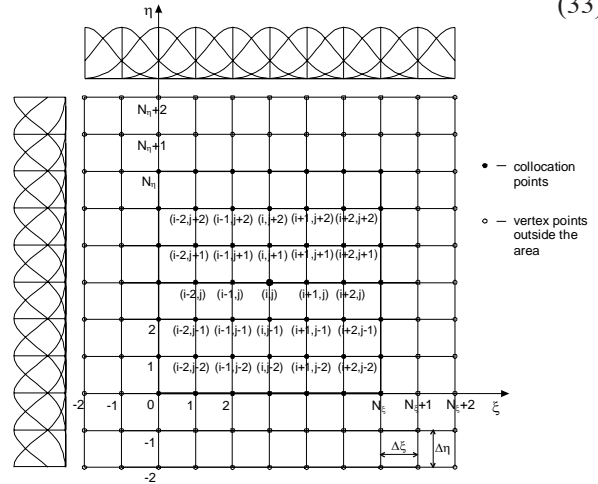


Fig. 21 Schematic presentation of approximate solution base

The numerical solution of the given problem by the FFCM is reduced to the search of  $C_{ij}$  unknown coefficients of a linear combination by solving the system of Eqs. (32) complete with respective boundary conditions. For a plate simply supported on all four edges, the boundary conditions are:

$$w(\xi, 0) = w(\xi, 1) = w(0, \eta) = w(1, \eta) = 0$$

$$\frac{\partial^2 w}{\partial \xi^2}(0, \eta) = \frac{\partial^2 w}{\partial \xi^2}(1, \eta) = \frac{\partial^2 w}{\partial \eta^2}(\xi, 0) = \frac{\partial^2 w}{\partial \eta^2}(\xi, 1) = 0 \quad (34)$$

For a plate clamped on all four edges, they are:

$$w(\xi, 0) = w(\xi, 1) = w(0, \eta) = w(1, \eta) = 0$$

$$\frac{\partial w}{\partial \xi}(0, \eta) = \frac{\partial w}{\partial \xi}(1, \eta) = \frac{\partial w}{\partial \eta}(\xi, 0) = \frac{\partial w}{\partial \eta}(\xi, 1) = 0 \quad (35)$$

Conditional equations at the corner of the plate are obtained by the Cartesian product of operators in boundary conditions on plate edges intersecting in that corner.

The numerical model has been tested on the example of a homogeneous isotropic thin square plate with a side length  $a$  and different boundary and loading conditions. The plate has been considered as one fragment. The obtained numerical results are compared in Table 4, with analytical solutions found in Ref. [9]. The presented method shows excellent correspondence with the exact results. As it can be seen in Table 4, the deviation of numerical values from the analytic ones is of the same order also for the deflection in the center of plate, which represents a main solution as well for bending moments

which are derived values.

Figure 22 shows bending moment  $M_{xx}$  and transverse force  $Q_x$  on a clamped uniformly loaded square plate. It can be observed that the boundary curves of the bending moment  $M_{xx}$  and the transverse force  $Q_x$  diagrams are extremely smooth which is the consequence of high smoothness of the applied basis functions, which also means that the boundary conditions are exactly satisfied.

Figure 23 shows distributions of the bending moment and transverse force on a clamped square plate loaded by a concentrated force in the middle. It can be concluded that the numerical solution obtained by FFCM accurately describes the real behaviour of the plate even in case of a concentrated load.

Table 4. Deflections and bending moments of the square plate with different boundary and loading conditions,  $\nu = 0.3$

Number of collocation points $(N+1) \times (N+1)$	Simply Supported Plate				Clamped Plate					
	uniform load $p$		central concentrated load $P$		uniform load $p$			central concentrated load $P$		
	Center deflection $w_{max}$	Moment at plate center $M_x$	Center deflection $w_{max}$	Moment at plate center $M_x$	Center deflection $w_{max}$	Moment at plate center $M_x$	Moment at side center $m_x$	Center deflection $w_{max}$	Moment at plate center $M_x$	Moment at side center $m_x$
$N = 4$	0.004284	0.05037	0.01127	0.19287	0.001312	0.02438	-0.04757	0.004833	0.1359	-0.1038
$N = 8$	0.004115	0.04848	0.01145	0.25896	0.001285	0.02335	-0.05012	0.005379	0.2049	-0.1181
$N = 16$	0.004075	0.04803	0.01155	0.32954	0.001271	0.02303	-0.05099	0.005542	0.2758	-0.1234
$N = 32$	0.004066	0.04792	0.01158	0.40098	0.001267	0.02294	-0.05124	0.005591	0.3473	-0.1251
$N = 40$	0.004064	0.04791	0.01160	0.42410	0.001266	0.02293	-0.05128	0.005598	0.3703	-0.1254
Analytic	0.004062	0.04790	0.01160	$\infty$	0.001260	0.02310	-0.05130	0.005600	$\infty$	-0.1257
Multiplier	$pa^4/D$	$pa^2$	$Pa^2/D$	$P$	$pa^4/D$	$pa^2$	$pa^2$	$Pa^2/D$	$P$	$P$

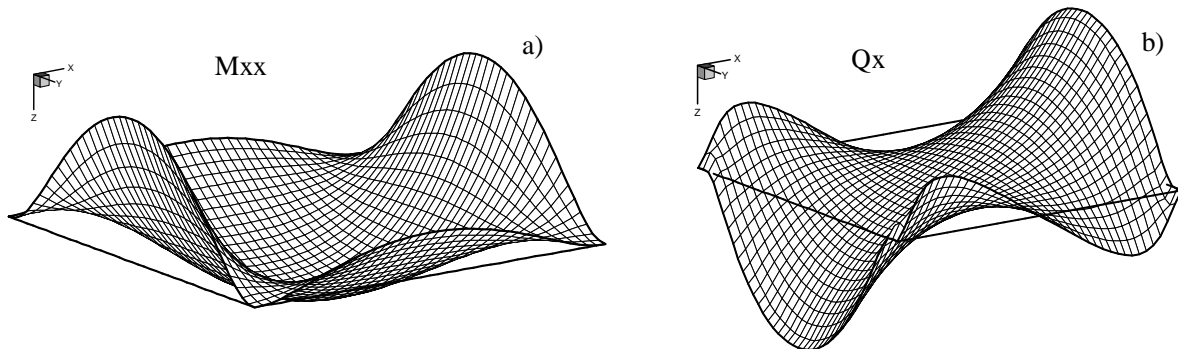


Fig. 22 Clamped plate under uniformly distributed load: a) Bending moment  $M_{xx}$ ; b) Transverse force  $Q_x$

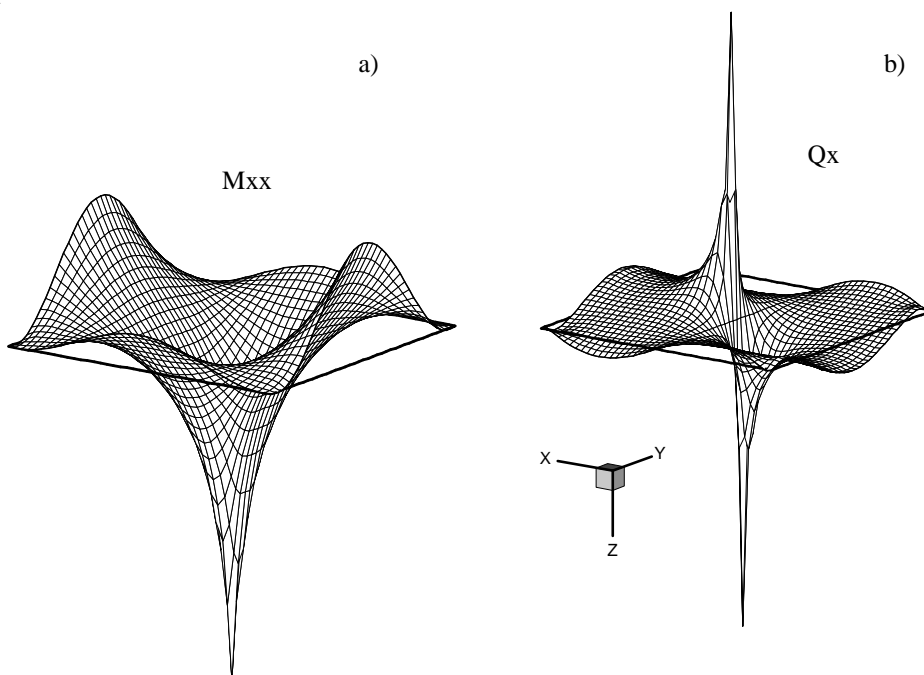


Fig. 23 Clamped square plate subjected to concentrated force in its middle: a) Bending moment  $M_{xx}$ ; b) Transverse force  $Q_x$

## 5. CONCLUSION

The numerical procedure of the fragment collocation method with basis functions  $Fup_n(x,y)$  is applied to the analyses of the torsion of prismatic bars, the plane stress and thin plate bending problems. The analyzed examples show that the numerical solution obtained by the FFCM converges monotonically towards an exact solution. The accuracy of the solution depends on the number of the collocation points i.e. on the number of basis functions in the domain and on the degree  $n$  of used basis functions  $Fup_n(x,y)$ . Because of the universality of the vector space formed by these functions, it is possible to hierarchically expand the number of basis functions in the domain which significantly accelerates the convergence of a numerical procedure in a simple way. By solving the given problem using the described method, the coefficients of a linear combination of basis functions  $C_{ij}$  are calculated for a selected number of collocation points. Once, when coefficients  $C_{ij}$  are obtained, the solution function values can be calculated with the same degree of accuracy as well as all values derived from the solution function in any point of the domain. Using the parametric formulation for the description of a given domain geometry the FFCM is adapted to analyses of curvilinear domains.

## 6. REFERENCES

- [1] V.L. Rvachev and V.A. Rvachev, On a finite function, *DAN URSR*. Ser. A, No. 6, pp. 705-707, 1971. (in Russian)
- [2] B. Gotovac, Numerical modelling of engineering problems by smooth finite functions, Ph.D. Thesis, Faculty of Civil Engineering, University of Zagreb, Zagreb, 1986. (in Croatian)
- [3] P.M. Prenter, *Splines and Variational Methods*, John Wiley & Sons, Inc., New York, 1989.
- [4] V. Kozulić, Numerical modeling by the fragment method with  $R_{bf}$  functions, Ph.D. Thesis, Faculty of Civil Engineering, University of Split, Split, 1999. (in Croatian)
- [5] V.L. Rvachev and V.A. Rvachev, *Non-classical Methods for Approximate Solution of Boundary Conditions*, Naukova dumka, Kiev, 1979. (in Russian)
- [6] F. Yamaguchi, *Curves and Surfaces in Computer Aided Geometric Design*, Springer-Verlag, Berlin, 1988.
- [7] A.I. Lurie, *Theory of Elasticity*, Nauka, Moskva, 1970.
- [8] K. Girkmann, *Flächentragwerke: Einführung in die elastostatik der scheiben, platten, schalen und faltwerke*, Springer-Verlag, Wien, 1959.
- [9] S.P. Timoshenko and S. Woinowsky-Krieger, *Theory of Plates and Shells*, 2<sup>nd</sup> edn, McGraw-Hill, New York, 1959.

## NUMERIČKA ANALIZA 2D PROBLEMA KORIŠTENJEM $Fup_n(x,y)$ BAZNIH FUNKCIJA

### SAŽETAK

U ovom radu prikazan je postupak numeričkog modeliranja dvodimenzionalnih inženjerskih problema korištenjem funkcija  $Fup_n(x,y)$ . To su finitne, beskonačno derivabilne funkcije koje pripadaju klasi Rvačevljevih baznih funkcija  $R_{bf}$ . Svojstva ovih funkcija omogućavaju hijerarhijski pristup povećavanju baze numeričkog rješenja, bilo na cijelom području, bilo na pojedinim njegovim dijelovima.

Približno rješenje problema pretpostavlja se u obliku linearne kombinacije baznih funkcija  $Fup_n(x,y)$ . Umjesto tradicionalne diskretizacije na konačne elemente, ovdje se cijelo područje može analizirati odjednom, kao jedan fragment. Metodom kolokacije formira se sustav jednadžbi u kojemu se u kolokacijskim točkama na zatvorenom području zadovoljava diferencijalna jednadžba problema, a na granici područja rubni se uvjeti zadovoljavaju egzaktno. Na ovaj se način jednostavno postiže zadana točnost približnog rješenja povećavanjem broja baznih funkcija. Pri tome se vrijednosti osnovne funkcije rješenja i sve veličine izvedene iz osnovnog rješenja izračunavaju u istim točkama budući da je izbjegnuta numerička integracija.

Metoda je testirana na problemima torzije prizmatičnih štapova, ravninskih stanja i savijanja tankih ploča. Rezultati analize uspoređeni su s postojećim egzaktnim i relevantnim numeričkim rješenjima. Može se zaključiti da kolokacijska metoda fragmenata, uz primjenu baznih funkcija  $Fup_n(x,y)$ , za obrađene probleme daje izvrsne rezultate, kako u pogledu točnosti, tako i u pogledu neprekinutosti svih polja izvedenih iz približnih rješenja.

**Ključne riječi:** približno rješenje, Rvačevljeve bazne funkcije, metoda kolokacije, fragment.